Chemical Physics Letters 657 (2016) 199–204

Contents lists available at ScienceDirect

Chemical Physics Letters

journal homepage: www.elsevier.com/locate/cplett

Research paper

Exploiting time-resolved magnetic field effects for determining radical ion reaction rates

A.O. Bessmertnykh [a,b], V.I. Borovkov [a,b,*], V.A. Bagryansky [a,b], Yu N. Molin [b]

[a] Novosibirsk State University, Pirogova, 2, 630090 Novosibirsk, Russia
[b] Institute of Chemical Kinetics and Combustion, SB RAS, Institutskaya, 3, 630090 Novosibirsk, Russia

ARTICLE INFO

Article history:
Received 22 April 2016
In final form 2 June 2016
Available online 4 June 2016

ABSTRACT

The capabilities of the method of time-resolved magnetic field effect in determining the rates of charge transfer reactions between radical ions and molecules on a nanosecond time scale have been investigated. The approach relies on the electron spin coherence in radical pair's partners generated by ionizing radiation. The spin evolution of the pair is sensitive to the reaction since the latter results in changing magnetic interactions of the unpaired electron. This process can be monitored by magnetic-field-sensitive fluorescence from an irradiated sample that is illustrated using reactions involving alkane radical cations. The accuracy and limitations of the approach are discussed.

1. Introduction

Charge transfer between radical ions (RIs) and molecules is a key process for a variety of reactions, occurring in chemical and biological systems. In order to study these charge transfer reactions, it is important to identify the radical ions involved, ideally, both the reactant and the product ones. However, the RIs of interest are frequently so reactive that observing them may be a considerable problem, which imposes great demands on the time resolution and sensitivity of the experimental technique applied.

In solutions, the most common technique for studying short-lived RIs and their reactions, is the pulse radiolysis technique to detect the transient optical absorption spectra of the irradiated matter. In favorable conditions, the technique allows one to follow transformations of the intermediates under study even on a picosecond time scale. Restrictions of the pulse radiolysis are concerned with the generation of a great variety of intermediates, typically, with broad overlapping absorption bands [1]. In particular, the pulse radiolysis is not selective to RIs, which carry both a charge and an unpaired electron spin, and fails to give information on the RI's structure comparable to that accessible with EPR technique.

The time-resolved techniques, based on the measuring of radiation-induced conductivity, are also used to study RIs transformations. These methods can be applied only when the charge carrier mobility changes significantly in the course of electron transfer reaction [2,3]. Similar to the pulse radiolysis, this approach fails to discriminate directly between RIs and a spinless charge carrier.

There are also time-resolved techniques based on the paramagnetic resonance phenomenon that are therefore specifically sensitive to free radicals. Direct detection of the resonance transitions in external magnetic fields with a time resolution of 10–30 ns can be realized with the time-resolved EPR technique (see, e.g. [4,5]) if the number of spins created in the sample per pulse is high enough. More sensitive approaches exploiting indirect EPR detection are the Pulsed Electrically Detected Magnetic Resonance [6,7] and the Optically or Fluorescence Detected Magnetic Resonance [8,9] methods that are capable, in principle, to provide a time resolution of tens of nanoseconds. Evidently, the mentioned approaches are hardly applicable to investigate charge transfer reactions that are completed on the time scale shorter than the time resolution of the methods.

This work was undertaken to expand the potentialities of one more approach to determining rates of the reactions involving short-lived radical ions. This is the method of time-resolved magnetic field effects (TR MFE) in recombination fluorescence [10,11], and its advantages originate from its selectivity with regard to radical ions as well as from a high temporal resolution inherent in optical measurements.

More precisely, the TR MFE method is sensitive to the spin-correlated radical ion pairs (RIPs), which arise in media under ionizing radiation. The recombination of these pairs in solution may result in fluorescence only if the spin state of the recombining RIP is singlet. The magnetic interactions between unpaired electron spins in the RIP's partners modulate the singlet state population of the pair thus modulating the kinetics of recombination

* Corresponding author at: Institute of Chemical Kinetics and Combustion, SB RAS, Institutskaya, 3, 630090 Novosibirsk, Russia.
E-mail address: borovkov@kinetics.nsc.ru (V.I. Borovkov).

http://dx.doi.org/10.1016/j.cplett.2016.06.011
0009-2614/

fluorescence. As the typical hyperfine coupling (HFC) constants in organic radical ions are of the order of 1 mT, the singlet–triplet transitions in RIPs occur usually in the nanosecond time domain. This makes the TR MFE method well suited for studying the short-lived RIs and for obtaining the same information on their characteristics as usually obtained by conventional EPR technique, namely, HFC constants, *g*-values, and paramagnetic relaxation times.

The charge transfer between one of the RIP partners and the charge acceptor from the bulk does not change spin correlation in a new RIP. However, the transfer is accompanied by the change in the magnetic interactions of one of the unpaired electrons, affecting the subsequent spin evolution of the pair. Thus, generally speaking, the recombination fluorescence intensity offers information on the change in the magnetic interactions of recombining short-lived RIs with time resolution and, as a result, on the charge transfer reactions, involving these particles.

This idea about the relation between the RIP spin state dynamics and chemical processes has been previously exploited in some particular cases for the RIs, having either negligible HFCs or very high relaxation rates (see below the discussion of Refs. [12–14]). The present work reports a more general case without serious limitations on EPR spectra characteristics for radical ionic species both decaying and arising in the course of the reaction. The possibilities of the approach are illustrated using electron transfer reactions involving radical cations (RCs) in low-viscosity alkane solutions.

2. Experimental and methodological details

2.1. Experimental

Recombination fluorescence from the *n*-hexane solutions studied was excited by ~1 ns pulses of X-rays with energy of about 20 keV and registered by single photon counting technique [15] in the fluorescence band of the *p*-terphenyl-d_{14} (*p*-TP-d_{14}) molecule ($\lambda_{max} \approx 360$ nm). This aromatic solute, *p*-TP-d_{14}, was used as an electron acceptor and luminophore at concentrations of about 30 μM. The rate constant for electron capture by the *p*-TP-d_{14} molecule in *n*-hexane is approximately 3×10^{12} M^{-1} s^{-1} [16], which is two orders of magnitude higher than that for encounter reactions between molecular species. Under these conditions, most of the recombination fluorescence is due to the recombination of the RIPs composed of the RC of the solvent (or the hole acceptor added to the solution) and the *p*-TP-d_{14} radical anion (RA). For the purposes of this work, it is important that HFC in the RA is comparatively small to provide a negligible contribution to the magnetic field effects in the time range studied. This allows focusing on the RCs under study.

Hexane was used as solvent since it has a high ionization potential and can be brought to a higher purity as compared to other compounds under study. To form the RCs of interest in the *n*-hexane solutions, we added the aliphatic compounds, 2,2,4,4,6,8,8-heptamethylnonane (HMN), 2,2,4-trimethylpentane (isooctane, isoOC), 2,6,10,15,19,23-hexamethyltetracosane (squalane, SQ), and *tris*(trimethylsilyl)amine (tTMSA) that are unlikely to affect the motion of solvated electrons in the *n*-hexane solutions in the concentration range studied. On the other hand, under our experimental conditions, all of these compounds serve as electron donors (hole acceptors). Indeed, according to the literature data, a positive charge should be transferred from the ionized *n*-hexane to the above-mentioned alkanes [14] and aliphatic amines like tTMSA [17,18].

To study the parallel, quasimonomolecular, irreversible decay of the charged reactant we have exploited the previously studied proton transfer reaction between the alkane RC and the 7-oxabicyclo[2,2,1]heptane (OCH) [19].

n-Hexane (99.8%, "Reactiv", Russia) and 2,2,4-trimethylpentane (Aldrich, 99.8%) were purified by passing through columns with activated alumina. 2,2,4,4,6,8,8-Heptamethylnonane (Aldrich, 98%), squalane (Aldrich, 99%), *tris*(trimethylsilyl)amine (Aldrich, 98%), 7-oxabicyclo[2,2,1]heptane (Aldrich, 98%), and *p*-terphenyl-d_{14} (Aldrich, 98%) were used as received.

To prevent the interaction of generated RIs and of excited luminophore molecules with dissolved oxygen, solutions were degassed by freeze–pump–thaw cycles. The temperature of irradiated samples was maintained at 20 °C.

The recombination fluorescence intensity decays, I_0 and I_B, were registered alternately in zero ($B < 0.05$ mT) and non-zero ($B = 0.1$ T) external magnetic fields, respectively. These fluorescence decay curves were used to calculate the ratio $I_B(t)/I_0(t)$, called the time-resolved magnetic field effect, for further analysis.

2.2. Basics of TR MFE technique

Delayed fluorescence from irradiated organic solutions of luminophores typically lasts much longer than the fluorescence of the singlet excited luminophore does. The reason for this is that some time passes before forming the electronically excited luminescent molecules due to the recombination of a RIP since the RIPs' partners diffuse to each other in the irradiated solution. Therefore, the decay of the intensity of recombination fluorescence depends on both the rate of the geminate RIP's recombination and the fluorescence lifetime of the excited luminophore. If the lifetime of the excited luminophore molecule is short enough, the radiative deactivation of the luminophore nearly coincides with the moment of the RIP recombination. As a result, the recombination fluorescence intensity, $I(t)$, is proportional to the recombination rate of the RIPs, $F(t)$, multiplied by the singlet state population of RIPs ensemble [10,11,20]:

$$I(t) \propto F(t) \cdot [\theta \rho_{SS}(t) + (1 - \theta)/4], \quad (1)$$

where $\rho_{ss}(t)$ is the time dependence of the singlet state population of the initially singlet-correlated RIPs. θ is a semiempirical parameter to take into account the fact that in the multiparticle radiation spur only a fraction of recombining RIPs is spin-correlated since some of them are composed of radical ions originating from the different primary ionization events. The second term in the brackets takes account of such spin-uncorrelated RIPs.

In this approximation, the TR MFE curve,

$$\frac{I_B(t)}{I_0(t)} = \frac{\theta \cdot \rho_{SS}^B(t) + (1 - \theta)/4}{\theta \cdot \rho_{SS}^0(t) + (1 - \theta)/4}, \quad (2)$$

depends only on the singlet state populations of the spin-correlated RIPs, $\rho_{ss}(t)$, in non-zero and zero external magnetic fields as indicated by superscripts *B* and 0, respectively. The $\rho_{ss}(t)$ dependence can be evaluated taking the paramagnetic relaxation into account as previously suggested [10,19]:

$$\rho_{ss}^B(t) = \frac{1}{4} + \frac{1}{4}\exp\left(-\frac{t}{T_1}\right) + \frac{1}{2}\exp\left(-\frac{t}{T_2}\right) G_c^B(t) G_a^B(t) \quad (3)$$

$$\rho_{ss}^0(t) = \frac{1}{4} + \frac{3}{4}\exp\left(-\frac{t}{T_0}\right) G_c^0(t) G_a^0(t) \quad (4)$$

where $1/T_{1,2} = 1/T_{(a)1,2} + 1/T_{(c)1,2}$ are the sums of the longitudinal and phase relaxation rates of RIP partners, and T_0 is the parameter to describe phase relaxation of the RIP in a zero magnetic field in the same manner. Subscripts "*a*" and "*c*" point to the parameters of RA and RC, respectively. Importantly, the analytical solutions to $G^0(t)$ are known only for some particular cases: the case of one or

two groups of equivalent magnetic nuclei and the case of a great number of nonequivalent nuclei (Appendix A).

If one of the RIP partners takes part in the electron transfer involving a neutral molecule so that this partner is transformed into another radical ion, then Eqs. (3) and (4) must be modified. Let us consider the reaction, which occurs at the moment t' and results in the transformation of a reactant, parent RC (denoted as $c1$) into another, secondary RC ($c2$). In this case, at a later time, $t > t'$, the singlet state population can be calculated as follows [21]:

$$\rho_{ss}^{B}(t,t') = \frac{1}{4} + \frac{1}{4}\exp\left(-\frac{t'}{T_1^{(c1)}}\right)\exp\left(-\frac{t-t'}{T_1^{(c2)}}\right) + \frac{1}{2}\exp\left(-\frac{t'}{T_2^{(c1)}}\right)exp\left(-\frac{t-t'}{T_2^{(c2)}}\right)G_{c1}^{B}(t')G_{c2}^{B}(t-t')G_{a}^{B}(t) \quad (5)$$

$$\rho_{ss}^{0}(t,t') = \frac{1}{4} + \frac{3}{4}\exp\left(-\frac{t'}{T_0^{(c1)}}\right)\exp\left(-\frac{t-t'}{T_0^{(c2)}}\right)G_{c1}^{0}(t')G_{c2}^{0}(t-t')G_{a}^{0}(t) \quad (6)$$

If the kinetics of the RC's reaction with bulk molecules can be described correctly using the rate constant k, the singlet state population averaged over t' with the exponential distribution at the moment t is of the form:

$$\rho_{ss}(t) = \exp(-kCt)\cdot\rho_{ss}(t,t) + kC\cdot\int_0^t \exp(-kCt')\rho_{ss}(t,t')dt'. \quad (7)$$

where C is the concentration of the added compound whose molecules form the secondary radical ions.

Eq. (7) allows one to consider more complicated forms of the kinetics of radical ions reactions too. This would be necessary when studying geminate recombination phenomena in amorphous solids, where bimolecular processes are described by a non-exponential kinetics (see, e.g. [22]), or studying TR MFE on a time scale of few nanoseconds for RIPs with comparatively large, say 10–20 mT [23], HFC constants, when time-dependent correction [24] for the rate constant should be taken into account.

3. Results and discussion

When analyzing the manifestation of phase coherences in the singlet–triplet transitions in a spin-correlated RIP, it is instructive to distinguish between the situations with the resolved and unresolved EPR spectra of the partners composing the RIP. If both the HFCs in RA and the RIPs' paramagnetic relaxation are insignificant, and the RC has the unresolved EPR spectrum, the corresponding TR MFE curve exhibits only one Gaussian-like peak [10,25]. Both the temporal width and the position of this peak are determined by the second moment of the EPR spectrum width, σ^2, of the RC. For the RC with magnetically equivalent nuclei, the TR MFE curve exhibits a series of distinct oscillations whose peak positions relate to the HFC constant. So, if the reactant RC shows the unresolved EPR spectrum and the reaction product RC exhibits the resolved one, these oscillations grow with increasing reaction rate. On the contrary, when the reactant RC with the resolved EPR spectrum is transformed into the RC with the unresolved one, this reaction reduces any oscillations in the spin state evolution of the RIP. In this work, we have studied these two cases of EPR spectrum transformation after the reactions denoted as "case A" and "case B", respectively. Below, these cases are considered using particular experimental systems. For case A, we also examine the accuracy of the approach and, besides, the applicability of this for estimating RI's reaction rates if such RI is involved in the parallel processes of quasi-monomolecular chemical decay.

3.1. Case A

To probe the sensitivity of the TR MFE curve to the transformation of RC with the unresolved EPR spectrum into that with the resolved one, we have studied the charge transfer reaction:

$$HMN^{+\cdot} + tTMSA \xrightarrow{k_8} HMN + tTMSA^{+\cdot} \quad (8)$$

The RC, $HMN^{+\cdot}$, having HFC with many magnetically nonequivalent protons and therefore showing the unresolved EPR spectrum, is transformed into $tTMSA^{+\cdot}$ with the dominant HFC constant with ^{14}N nucleus. The HFC constant, $a(^{14}N)$ = 1.2 mT, was obtained from our TR MFE experiments. We have also determined the value σ = 1.5 mT as the EPR spectrum width of $HMN^{+\cdot}$ which is close to 1.6 mT, obtained in Ref. [14].

To ensure a fast trapping of the primary hexane holes by HMN molecules we have used a rather high HMN concentration of 0.1 M. Assuming that the trapping is the diffusion-controlled reaction with a rate constant of about $3–4 \times 10^{10}$ M^{-1} s^{-1} [19], we have estimated the characteristic trapping time as ~0.1 ns, which is much shorter than an instrument response function of ≈1 ns. The concentration of tTMSA was chosen low enough from 1 to 3 mM to prevent the formation of $tTMSA^{+\cdot}$ due to the direct trapping of solvent holes. Note that within our 100 ns observation window we can neglect a positive charge transfer from any molecular RCs to p-TP-d_{14} molecules.

Fig. 1a shows the transformation of TR MFE curves with increasing tTMSA concentrations. There is only one distinct peak with its maximum at times less than 10 ns in the absence of the solute. As the tTMSA concentration increases, the additional oscillations caused by the HFC of unpaired electron with ^{14}N nucleus in tTMSA RC become apparent.

The simulation of the experimental curves using Eqs. (2), and (5)–(7) showed that the best fit was reached with the rate constant $k_8 = 4.0 \times 10^{10}$ M^{-1} s^{-1}. This value is very close to the reaction rate constants of positive charge transfer from $HMN^{+\cdot}$ to other amines, $(3.5–3.7) \times 10^{10}$ M^{-1} s^{-1}, as determined in the n-hexane solutions in Ref. [19]. To show the accuracy of the TR MFE method, Fig. 1b depicts the fittings of the curve with 1.5 mM tTMSA at the rate constants $k_8 = 4 \times 10^{10}$ M^{-1} s^{-1} varied by 30% up and down which makes the fit to experiment less satisfactory.

With the use of the system, where reaction (8) occurs, we have also verified the applicability of the TR MFE method for estimating the rate of the reaction between RI and molecule when the RI is involved in the parallel quasi-monomolecular chemical reaction resulting in quenching of recombination fluorescence. The fact is that the fragmentation or intermolecular proton transfer involving the alkane radical cations are often mentioned as such reactions [1,8]. To model these, we have added ether, OCH, to the irradiated solution of HMN and tTMSA in n-hexane. The reaction

$$HMN^{+\cdot} + OCH \xrightarrow{k_9} Products \quad (9)$$

has been previously studied by the method of pre-recombinational quenching [19], which allows us to compare the results obtained by these two methods. As suggested in the work cited, the OCH molecules react with $HMN^{+\cdot}$ without a subsequent formation of luminescence states due to intermolecular proton transfer.

Fig. 2a and b exemplify the effect of adding 3 mM OCH to the n-hexane solution of 0.1 M HMN, 1 mM tTMSA and 30 μM p-TP-d_{14}. Fig. 2a shows a drastic relative acceleration of the fluorescence intensity decay as a result of the OCH addition that is in accordance with the previous results [19]. Note that at $t > 20$ ns the fluorescence intensity decay for both of the curves presented is of a hyperbolic form, which is typical of geminate recombination. This indicates [26] OCH to react only with $HMN^{+\cdot}$ and not to react with $tTMSA^{+\cdot}$. Therefore, due to reaction (9) the reactant RC, $HMN^{+\cdot}$, is

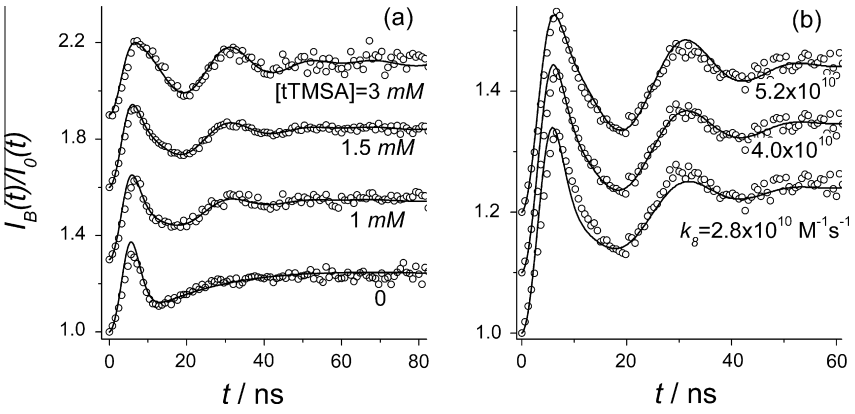

Fig. 1. (a) Experimental (circles) and calculated curves of TR MFE in recombination fluorescence of 0.1 M HMN, 30 μM *p*-TP-d_{14} in *n*-hexane solution with varied concentrations of tTMSA (shown in the graph). The modeling was performed with the reaction rate constant $k_8 = 4 \times 10^{10}$ M^{-1} s^{-1}. (b) The same for solution with 1.5 mM tTMSA using simulation with the *k* value varied by 30% up and down as indicated in the plot. The curves are shifted vertically.

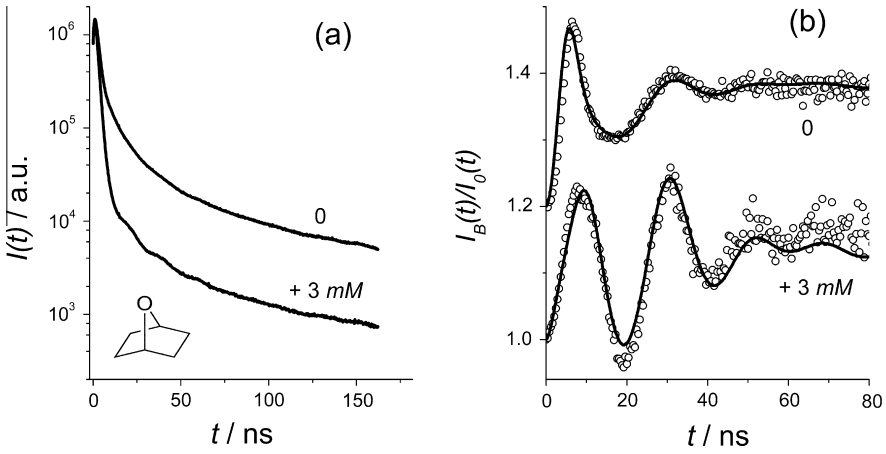

Fig. 2. (a) Delayed fluorescence decays from *n*-hexane solution of 0.1 M HMN, 1 mM tTMSA and 30 μM *p*-TP-d_{14} without (upper curve) and with 3 mM OCH (bottom curve). (b) Experimental (circles) and calculated (lines) ratios of fluorescence intensities in high and zero magnetic fields of the same solution without (upper curve) and with OCH (bottom curve). The calculation was performed at the reaction rate constants $k_8 = 3.4 \times 10^{10}$ M^{-1} s^{-1}, $k_9 = 3.7 \times 10^{10}$ M^{-1} s^{-1}. For convenience, the curves are shifted vertically.

actually removed from the ensemble probed by the observation of recombination fluorescence via two approximately independent pathways.

The presence of the parallel reaction path requires a slight modification of Eq. (7). The decay of $HMN^{+\cdot}$ due to reactions (8) and (9) can be described using the equation of formal chemical kinetics,

$$\frac{d[HMN^{+\cdot}]}{dt} = -(k_8[t\text{TMSA}] + k_9[\text{OCH}]) \cdot [HMN^{+\cdot}] \qquad (10)$$

Thus, by analogy with Ref. [26], the exponential distribution of the primary RIP lifetimes used in Eq. (7) with the characteristic time $\tau_8 = 1/(k_8 \cdot [\text{tTMSA}])$ should be replaced in the case of two competing reactions (8) and (9), by the reduced time $\tau_8\tau_9/(\tau_8 + \tau_9)$, where $\tau_9 = 1/(k_9 \cdot [\text{OCH}])$.

Adding the quencher, OCH, makes the oscillations, observed on the curve of the recombination fluorescence decay, prominent (Fig. 2a). The TR MFE curves show a manifestation of quantum beats more clearly (Fig. 2b). The increase in peaks' amplitudes due to the presence of parallel reaction (9) can be attributed to a decrease in both the characteristic time and the formation time spread for $tTMSA^{+\cdot}$, whose recombination with RA results in the fluorescence observed.

In the simulation shown in Fig. 2b, we have used the rate constant of reaction (9), $k_9 = 3.7 \times 10^{10}$ M^{-1} s^{-1} determined previously [19]. The best fit to the experiment, with the use of formulas (2), and (5)–(7) to simulate the curves of TR MFE in Fig. 2b, was reached with the rate constant of reaction (8) $k_8 = 3.4 \times 10^{10}$ M^{-1} s^{-1}. Taking the estimated accuracy of the TR MFE method into account, this result agrees fairly well with the value obtained in the experiment without OCH. This example also suggests that studies on the concentration dependence of the TR MFE curves allow one to determine the rates of both parallel processes though with a reduced accuracy.

3.2. Case B

The charge transfer with transition from RC with the resolved EPR spectrum to RC with the unresolved one is exemplified by the reaction

$$\text{isoOC}^{+\cdot} + \text{SQ} \xrightarrow{k_{11}} \text{isoOC} + \text{SQ}^{+\cdot}, \qquad (11)$$

where the reactant RC, $isoOC^{+\cdot}$, is transformed into $SQ^{+\cdot}$, having HFCs with many magnetically nonequivalent nuclei. The best fit to the experiments (Fig. 3) is reached by describing HFC in $isoOC^{+\cdot}$ with two groups of equivalent protons with the constants $a(10H) = 1.25$ mT and $a(6H) = 0.37$ mT. These values are very close to 1.3 mT (10H) and 0.37 mT (6H) that were determined in Ref. [14]; $SQ^{+\cdot}$ is considered as a particle with the unresolved EPR spectrum

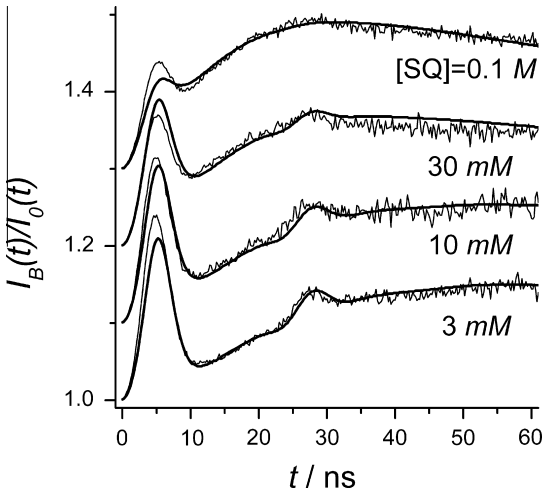

Fig. 3. Experimental (noisy) and calculated (smooth) ratios of fluorescence intensities in high, 0.1 T, and zero magnetic fields for *n*-hexane solution of 0.3 M isoOC, 30 μM *p*-TP-d_{14} and SQ, whose concentrations are shown in the figure. The modeling was performed with the rate constant of reaction (11), $k_{11} = 1 \times 10^9$ M^{-1} s^{-1}, with DEE rate constant, $k_{ex} = 1.0 \times 10^9$ M^{-1} s^{-1}, for SQ RC. For convenience, the curves are shifted vertically.

with $\sigma = 0.4$ mT [14]. Additionally, the degenerate electron transfer, involving RC and SQ molecules, was taken into account within the approach described in Appendix A.

As before, we have used a rather high isoOC concentration of 0.3 M. A further increase in concentration did not change the TR MFE curves, which indicates that the charge transfer from ionized hexane to the isoOC molecule occurs almost instantly to prevent any contributions of solvent holes to the TR MFE. When SQ is added at lower concentrations, the charge transfer reaction (11) occurs that causes a decrease in the amplitudes of the peaks related to $isoOC^{+\cdot}$ (Fig. 3). The best fit to the experimental curves is reached with the reaction rate constant $k_{11} = 1.0 \times 10^9$ M^{-1} s^{-1}, which is by an order of magnitude less than the diffusion controlled reaction rate constant. Such a low value explains a negligible effect of SQ at its concentration of about 3 mM (Fig. 3). To achieve better fits at higher SQ concentrations, in addition to reaction (11) it is necessary to account for the degenerate electron exchange (DEE) between molecules and RCs of squalane (Appendix A) with the similar rate constant $k_{ex} \approx 1.0 \times 10^9$ M^{-1} s^{-1}.

The reason for such low rates of both reaction (11) and the DEE, involving the SQ RCs, is very probably the same as that suggested previously for the DEE reaction involving the *n*-alkane RCs [13]. It was shown that the ionization potential of the alkane molecule with a long carbon skeleton increases for conformations of *n*-alkane formed by rotation of the fragments of the initial *all-trans* structure around the C–C bond of the skeleton. As the probability to be in the conformation with multiple *gauche* transitions is relatively high for long SQ molecules in solution, they supposedly do not participate in reaction (11) of electron transfer to the isoOC RC. This results in a decrease of the effective reaction rate constant as compared with that of reagent encounters in solution.

3.3. Capabilities and restrictions of the TR MFE method

As mentioned in the Section 1, the method of TR MFE in recombination fluorescence has already been applied to investigate ion-molecular reactions in some particular cases. The results of ion-molecular reaction rate measurements are summarized in Table 1.

For the first time, the above approach was used to estimate the rate of charge transfer between the $isoOC^{+\cdot}$ and diphenylsulfide-d_{10} (DPS-d_{10}) molecules [12]. The damped harmonic oscillations caused by the difference between the g-factors of the DPS-d_{10} RC and *p*-TP-d_{14} RA were observed on the TR MFE curves. The rate constant was obtained from oscillation phase shift, caused by the time delay of DPS-d_{10} RC formation. Actually, this approach can be applied only to the simplest case where the EPR spectra of RIP partners are the narrow singlets. In particular, since $isoOC^{+\cdot}$ exhibits a broad EPR spectrum, a more complicated theoretical analysis is needed to get better estimates.

Table 1
The charge transfer rate constants determined by the TR MFE technique.

Reaction[a]	Rate constant, M^{-1} s^{-1}	Reference
$isoOC^{+\cdot} + DPS\text{-}d_{10} \rightarrow isoOC + DPS\text{-}d_{10}^{+\cdot}$	$(3.5 \pm 1) \times 10^{10}$[b]	[12]
$C_9H_{20}^{+} + C_9H'_{20} \rightarrow C_9H_{20} + C_9H'^{+\cdot}_{20}$	$(2.6 \pm 0.4) \times 10^{8}$[c]	[13]
$C_{12}H_{26}^{+} + C_{12}H'_{26} \rightarrow C_{12}H_{26} + C_{12}H'^{+\cdot}_{26}$	$(1.6 \pm 0.2) \times 10^{8}$[c]	[13]
$C_{16}H_{34}^{+} + C_{16}H'_{34} \rightarrow C_{16}H_{34} + C_{16}H'^{+\cdot}_{34}$	$(2.8 \pm 0.6) \times 10^{8}$[c]	[13]
$isoOC^{+\cdot} + DMA \rightarrow isoOC + DMA^{+\cdot}$	$(1.5 \pm 0.2) \times 10^{10}$[c]	[14]
$isoOC^{+\cdot} + t\text{-}DEC \rightarrow isoOC + t\text{-}DEC^{+\cdot}$	$(1.0 \pm 0.2) \times 10^{10}$[c]	[14]
$NB^{+\cdot} + NB' \rightarrow NB + NB'^{+\cdot}$	$(1.5 \pm 0.3) \times 10^{10}$[c]	[29]
$HMN^{+\cdot} + tTMSA \rightarrow HMN + TMSA^{+\cdot}$	$(4.0 \pm 0.6) \times 10^{10}$[c]	This work
$isoOC^{+\cdot} + SQ \rightarrow isoOC + SQ^{+\cdot}$	$(1 \pm 0.3) \times 10^{9}$[c]	This work

[a] isoOC = isooctane; DPS-d_{10} = diphenylsulfide-d_{10}; DMA = 1,3-dimethyladamantane; *t*-DEC = *trans*-decalin; HMN = 2,2,4,4,6,8,8-heptamethylnonane; NB = norbornane; tTMSA = *tris*(trimethylsilyl)amine; SQ = squalane.
[b] Solvent = isooctane.
[c] Solvent = *n*-hexane.

Another particular case was considered by Potashov and coworkers [14], who studied the positive charge transfer from $isoOC^{+\cdot}$ to the particles, forming RCs with very short spin–lattice relaxation times, T_1. In that case, the rate of the observed long-time decay of the TR MFE curves was almost equal to the reaction rate. 1,3-Dimethyladamantane and *trans*-decalin were chosen as positive charge acceptors whose RCs have very short relaxation times, $T_1 \sim 6$ ns [27] and $T_1 \sim 10$ ns [28], respectively. Modeling the TR MFE curves showed that the rate of electron transfer from the molecules of these cyclic alkanes to $isoOC^{+\cdot}$ RC is determined by reactants diffusion.

The TR MFE technique was also successfully applied to study the alkane RCs DEE. Note that only this approach can be used in the nanosecond time domain because the optical absorption spectra do not change in these reactions while the HFCs are modulated causing changes in the TR MFE curves. To estimate the DEE rate for the *n*-alkane RCs with a comparatively narrow EPR spectrum width in solutions, it was necessary to model the TR MFE curves within the time range where the phase coherence was not lost yet [13]. On the contrary, studying the DEE reaction for norbornane RC in the *n*-hexane solutions required the analysis of the magnetic field dependences of the long-time tails of the TR MFE curves, determined exclusively by the spin–lattice relaxation process [29]. Unlike the *n*-alkane RCs electron self-exchange reaction, for the norbornane RC, which seems to exhibit a rigid structure, the self-exchange may occur at almost every encounter between the RC and neutral molecules in solutions.

Examples, summarized in Table 1, show that the TR MFE method can be applied to determine the rate constants of various ion-molecular reactions. Under favorable conditions, the achievable precision of the measurement is better than 30% that depends, in particular, on the magnetic characteristics of radical ionic species before and after reaction.

As any other approach, the TR MFE method has its own limitations. To observe recombination fluorescence kinetics, a luminophore is required with the fluorescence time significantly shorter than the characteristic times of the processes studied. It is very desirable that the partner of the radical ion of interest would have a narrow EPR spectrum in order to minimize its contribution to the spin evolution of the RIP studied. The capabilities of the TR MFE

method are also limited if the primary radical ion exhibits very fast paramagnetic relaxation. When the transverse relaxation time T_2 is shorter than the characteristic time of chemical reaction and the longitudinal relaxation time T_1 is substantially longer than T_2, the method remains to be applicable but its precision decreases because the short T_2 causes a fast singlet–triplet mixing and the peculiarities of the curve become less apparent. When both T_1 and T_2 are significantly shorter than the chemical reaction time, the TR MFE method becomes uninformative.

4. Conclusions

In this work, we have verified that the method of time-resolved magnetic field effect in recombination fluorescence from irradiated solutions can be used to determine the rates of ion-molecular reactions involving one of the partners of the spin-correlated RIP. The applicability of the approach was tested for the positive charge transfer reactions resulting in the transformation of the unresolved EPR spectrum into the resolved one (case A) and vice versa (case B). For case A, the inherent accuracy of the approach was estimated and its usefulness was tested in the case of RI involvement in the parallel reaction of chemical decay. It was shown that the available theoretical model allows a reasonable reproduction of the experimental TR MFE curves in the nanosecond time domain.

Acknowledgement

This work was supported by Russian Foundation for Basic Researches (RFBR, Grant 14-03-01046).

Appendix A

The analytical solutions to $G^{0,B}(t)$ are known only for some particular cases: the case of some equivalent magnetic nuclei groups and the case of the great number of nonequivalent magnetic nuclei. For a great amount of magnetic nuclei with the different HFC constants (particles with the unresolved EPR spectrum), in the framework of semi-classical approximation functions $G(t)$ have the forms (in the field units for σ and a) [25],

$$G^0(t) = \frac{1}{3}\cdot[1 + 2\cdot(1-(\gamma\sigma t)^2)\cdot\exp(-(\gamma\sigma t)^2/2)], \tag{A1}$$

$$G^B(t) = \exp[-(\gamma\sigma t)^2/2], \tag{A2}$$

where σ^2 is the second momentum of the radical ion EPR spectrum, γ is the electron gyromagnetic ratio.

For a one magnetic nucleus with spin I and the HFC constant a [10,20],

$$G^0(t) = \frac{3 + 4I(I+1)\cdot(1 + 2\cdot\cos(\gamma a(I+1/2)\cdot t))}{3(2I+1)^2}, \tag{A3}$$

$$G^B(t) = \frac{1}{2I+1}\cdot\frac{\sin(\gamma a(I+1/2)\cdot t)}{\sin\left(\gamma\frac{a}{2}\cdot t\right)}. \tag{A4}$$

The spin evolution can be described by taking account of the degenerate electron exchange (DEE) causing multiple accidental changes in nuclear projections [25]. If one of the RIP partners participates in the DEE, its $G(t)$ functions should be replaced by the following ones

$$\Gamma_c(t) = \sum_{n=1}^{n=\infty} G_c^{(n)}(t), \tag{A5}$$

where the term

$$G_c^{(n)}(t) = \tau^{-1}\cdot\int_0^t G_c^{(1)}(t')\cdot G_c^{(n-1)}(t-t')dt' \tag{A6}$$

allows for an accidental realization of $(n-1)$ acts of charge exchange by moment t.

$$G_c^{(1)}(t) = G_c(t)\cdot\exp(-t/\tau), \tag{A7}$$

τ_c is the average time of electron exchange.

References

[1] R. Mehnert, Radical cation in pulse radiolysis, in: A. Lund, M. Shiotani (Eds.), Radical Ionic Systems, Kluwer Academic Publishers, Dodrecht, The Netherlands, 1991, pp. 231–284.
[2] W.F. Schmidt, Liquid State Electronics of Insulating Liquids, CRC Press, Boca Raton, Florida, 1997.
[3] J.M. Warman, M.P. De Haas, Time-resolved conductivity techniques, DC to microwave, in: Y. Tabata (Ed.), Pulse Radiolysis, CRC Press, Boca Raton, Florida, 1991, pp. 101–133.
[4] R. Bittl, S. Weber, Biochim. Biophys. Acta 1707 (2005) 117.
[5] Q. Mi, M.A. Ratner, M.R. Wasielewski, J. Phys. Chem. A 114 (2010) 162.
[6] C. Boehme, D.R. McCamey, K.J. van Schooten, et al., Phys. Stat. Solidi B 246 (2009) 2750.
[7] J.M. Lupton, D.R. McCamey, C. Boehme, Chem. Phys. Chem. 11 (2010) 3040.
[8] A.D. Trifunac, D.W. Werst, in: A. Lund, M. Shiotani (Eds.), Radical Ionic Systems, Kluwer Academic Publishers, Dordrecht, The Netherlands, 1991, pp. 195–230.
[9] Y. Kitahama, Y. Sakaguchi, J. Phys. Chem. A 112 (2008) 347.
[10] V.A. Bagryansky, V.I. Borovkov, Yu N. Molin, Russ. Chem. Rev. 76 (2007) 493.
[11] V. Borovkov, D. Stass, V. Bagryansky, Y. Molin, Study of spin-correlated radical ion pairs in irradiated solutions by optically detected EPR and related techniques, in: A. Lund, M. Shiotani (Eds.), Applications of EPR in Radiation Research, Springer International Publishing, New York, 2014, pp. 629–663.
[12] V.M. Grygoryants, B.M. Tadjikov, O.M. Usov, Yu N. Molin, Chem. Phys. Lett. 246 (1995) 392.
[13] V.I. Borovkov, N.P. Gritsan, I.V. Yeletskikh, et al., J. Phys. Chem. A 110 (2006) 12752.
[14] P.A. Potashov, V.I. Borovkov, L.N. Shchegoleva, et al., J. Phys. Chem. A 116 (2012) 3110.
[15] S.V. Anishchik, V.M. Grigoryantz, I.V. Shebolaev, et al., Prib. Technol. Eksp. 4 (1989) 74 (in Russian).
[16] J.A. Crumb, J.K. Baird, J. Phys. Chem. 83 (1979) 1130.
[17] S.M. Lefkowitz, A.D. Trifunac, J. Phys. Chem. 88 (1984) 77.
[18] V.M. Grigoryants, O.A. Anisimov, Yu N. Molin, J. Struct. Chem. 23 (1982) 327.
[19] V.I. Borovkov, K.A. Velizhanin, Chem. Phys. Lett. 4 (2004) 441.
[20] V.A. Bagryansky, V.I. Borovkov, Y.N. Molin, Phys. Chem. Chem. Phys. 6 (2004) 924.
[21] V.A. Bagryansky, O.M. Usov, N.N. Lukzen, et al., Appl. Magn. Reson. 4 (1997) 505.
[22] L. Berthier, G. Biroli, J.-P. Bouchaud, L. Cipelletti, W. van Saarloos (Eds.), Dynamical Heterogeneity in Glasses, Colloids and Granular Media, Oxford University Press, Oxford, 2011.
[23] V.I. Borovkov, I.V. Beregovaya, L.N. Shchegoleva, et al., J. Phys. Chem. A 119 (2015) 8443.
[24] S.A. Rice, Diffusion-Limited Reactions, Elsevier, Amsterdam, 1985.
[25] K. Schulten, P.G. Wolynes, J. Chem. Phys. 7 (1978) 3292.
[26] V.I. Borovkov, I.S. Ivanishko, Radiat. Phys. Chem. 4 (2011) 540.
[27] V.I. Borovkov, Y.N. Molin, Chem. Phys. Lett. 398 (2004) 422.
[28] V.I. Borovkov, Y.N. Molin, Phys. Chem. Chem. Phys. 6 (2004) 2119.
[29] V.I. Borovkov, K.L. Ivanov, V.A. Bagryansky, Y.N. Molin, J. Phys. Chem. A 110 (2006) 4622.